Ultrahigh magnetic field spectroscopy reveals the band structure of the 3D topological insulator Bi_2Se_3

A. Miyata,[1] Z. Yang,[1] A. Surrente,[1] O. Drachenko,[1] D. K. Maude,[1] O. Portugall,[1] L. B. Duffy,[2] T. Hesjedal,[2] P. Plochocka,[1] and R. J. Nicholas[2,*]

[1] *Laboratoire National des Champs Magnetiques Intenses, CNRS-UGA-UPS-INSA, 143 Avenue de Rangueil, 31400 Toulouse, France*

[2] *Clarendon Laboratory, University of Oxford, Parks Road, Oxford, OX1 3PU, UK*

(Dated: June 6, 2017)

We have investigated the band structure at the Γ point of the three-dimensional (3D) topological insulator Bi_2Se_3 using magneto-spectroscopy over a wide range of energies ($0.55-2.2$ eV) and in ultrahigh magnetic fields up to 150 T. At such high energies ($E > 0.6$ eV) the parabolic approximation for the massive Dirac fermions breaks down and the Landau level dispersion becomes nonlinear. At even higher energies around 0.99 and 1.6 eV, new additional strong absorptions are observed with a temperature and magnetic-field dependence which suggest that they originate from higher band gaps. Spin orbit splittings for the further lying conduction and valence bands are found to be 0.196 and 0.264 eV.

Topological insulators, which have a finite insulating bandgap in the bulk form, but which can become gapless at the surface, have been intensively investigated as a new class of quantum matter.[1–3] Their surface states have topologically-protected Dirac fermions with spins locked to their translational momentum due to a strong spin-orbit coupling, giving them considerable potential to be used in future electronic and spintronic devices.[4,5] The experimental observation of a single Dirac cone in the surface state by angle-resolved photoemission spectroscopy (ARPES) was reported for Bi_2Se_3,[6,7] Bi_2Te_3[8] and Sb_2Te_3,[9] confirming that they are three-dimensional (3D) topological insulators with large bandgap in the bulk (0.1–0.3 eV). This observation stimulated a large body of work to investigate the unconventional properties arising from the topological surface states. However, there have been few experimental studies of their band structures in the bulk, despite the fact that the origin of topological surface states is critically dependent on the band inversion in the bulk crystal. In Bi_2Se_3, the bulk band structure has been described using a massive Dirac Hamiltonian with a negative mass parameter caused by band inversion due to strong spin-orbit coupling.[10,11] While ARPES studies have reported the existence of a camelback-like band structure at the Γ point "near the surface" of Bi_2Se_3 consistent with the band inversion in the bulk,[7] other techniques such as magneto-transport and infrared spectroscopy favor a bulk behavior with a direct bandgap at the Γ point (*i.e.* no camelback-like structure).[12,13] The latter results are supported by theoretical *GW* calculations[14,15] which suggest that electron-electron interactions suppress the camelback-like structure in the bulk bands of Bi_2Se_3.

Magneto-optical studies recently revealed the band character in the bulk of Bi_2Se_3, which has been described by a massive Dirac Hamiltonian with a negative mass term.[16] Remarkably, the observed evolution of the Landau-level energies in Bi_2Se_3 remain linear even up to 32 T, indicating that for the energies investigated ($E < 0.6$ eV), the band dispersion in the bulk of Bi_2Se_3 is almost perfectly parabolic. The *GW* calculations[14,15] have suggested the existence of higher direct bandgaps at the Γ point, in the near infrared and visible range. The higher conduction and valence band can influence carriers in the lower bands, especially in the presence of an applied magnetic field. To date only limited evidence of the higher band transitions has been presented[17] from fitting of the dielectric function at room temperature.

In this paper, we present magneto-optical studies of single crystal thin-film Bi_2Se_3 using ultrahigh magnetic fields up to 150 T over a wide range of energies (0.55 to 2.2 eV). The single crystal thin films are grown on *c*-plane sapphire substrates using molecular beam epitaxy, as described in detail in Refs.18 and 19. We reveal the nonlinear magnetic-field evolution of the Landau levels of fundamental bands in the bulk form of Bi_2Se_3, which is explained by the massive Dirac model with the negative mass term. At high energies, ∼0.99 and 1.6 eV, additional strong absorptions are observed. From their temperature and magnetic-field dependence, they are assigned as the lowest interband Landau level transitions of 2^{nd} and 3^{rd} bandgaps, respectively.

Figure 1(a) shows representative differential (normalized by dividing by zero-field spectra) transmission spectra, $T(B)/T(0)$, in Bi_2Se_3 taken at 35, 47, 60 and 67 T which reveal a number of well resolved absorption minima. At energies below 0.95 eV, we observe features due to inter Landau level absorption across the direct gap (transitions labeled E_1) at the Γ-point. To study these absorptions in detail we performed magnetic field dependent measurements up to 150 T, using an explosive single turn coil and single frequency sources .[20] Figure 1(b) shows normalized magneto-transmission, $T(B)/T(0)$, of Bi_2Se_3 for excitation energies of 0.775, 0.800, 0.810 and 0.886 eV around $T = 7$ K up to 150 T. The transmission minima denoted by triangular symbols in Fig. 1(b) show clear shifts to higher magnetic fields with increasing energies, which correspond to the interband Landau level

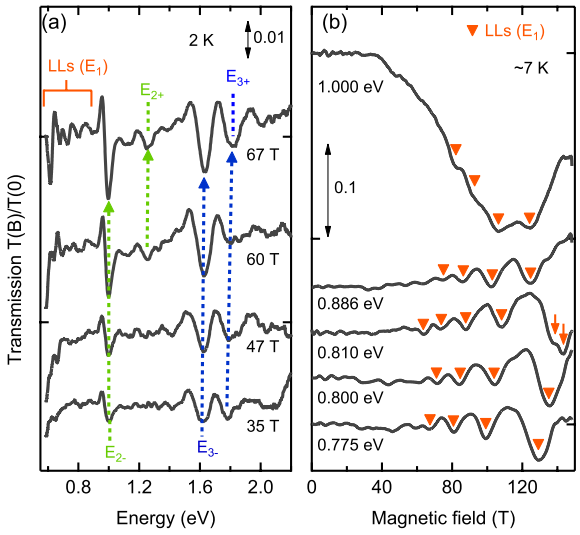

FIG. 1. (a) Low-temperature differential transmission spectra of Bi_2Se_3 at different magnetic fields of 35, 47, 60 and 67 T. (b) Magneto transmission of Bi_2Se_3 at different energies at 7 K. (a, b) Spectra were shifted vertically for clarity.

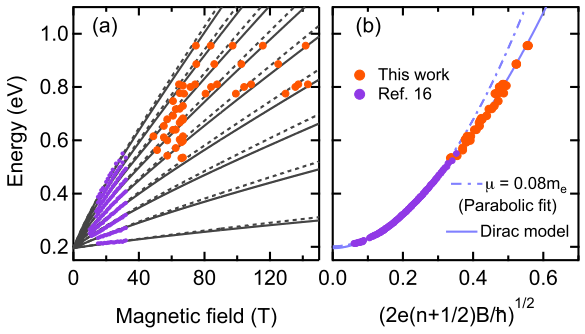

FIG. 2. (Color online) (a)Low-temperature interband Landau level fan chart for 1st (fundamental) bandgap in Bi_2Se_3. Dashed and solid lines are interband Landau levels obtained by the 4×4 massive Dirac Hamiltonian with the electron-hole asymmetry. (b)Energy-momentum dispersion of Bi_2Se_3. Broken line shows the fitting for parabolic dispersion. Inset shows the deviation from the parabolic dispersion.

transitions of the fundamental band gap (∼0.2 eV) in the bulk of Bi_2Se_3[16].

Figure 2(a) shows the Landau level fan chart combining our transmission data with the low-energy data of Orlita *et al.*.[16] The dipole allowed ($\Delta n = \pm 1$) interband inter Landau levels transitions, calculated using the 4×4 massive Dirac Hamiltonian[10,11] reproduce the data perfectly, with a band gap of 2Δ=0.19 eV, Fermi velocity $v_D = (0.465 \pm 0.05) \times 10^6$ ms^{-1}, negative mass term $M = -(17\pm0.5)\,\mathrm{eV\AA}^2$. The electron-hole asymmetry parameter $C = (3 \pm 0.5)$ eVÅ^2, which reflects the different electron and hole effective masses, was determined from the observed splitting of interband Landau level transition, indicated by arrows in Fig. 1(b).

Our fitting parameters are identical within experimental error with those obtained by Orlita *et al.*,[16] with the important exception of the negative mass term. Our higher energy data places stronger constraints on the value of M and our value of $|M| = 17\,\mathrm{eV\AA}^2$ is roughly 25% smaller than found by fitting to the low energy data of Orlita *et al.*. This implies that the condition $\hbar^2 v_D^2 = -4M\Delta$ required in the Dirac model to have a strictly parabolic dispersion over a wide energy range, is not fulfilled as well as previously thought. We have $\hbar^2 v_D^2 \simeq 9.6\,\mathrm{eV^2\AA}^2$ but with a significantly smaller value for $-4M\Delta \simeq 6.8\,\mathrm{eV^2\AA}^2$. This also has implications for the magnetic field $B_c = \hbar\Delta/|eM|$ at which the $n = 0$ Landau levels of the conduction and valence bands cross. The lower value of $|M|$ found here shifts B_c to higher magnetic field ($B_c \simeq 390$ T compared to the value of around 300 T estimated by Orlita *et al.*).

In Fig. 2(b), the experimentally obtained inter band Landau level transition energies, with different indexes are scaled into the same energy-momentum dispersion of Bi_2Se_3, deduced from the relation between the momentum k and magnetic field B. Neglecting electron hole asymmetry, and assuming a parabolic dispersion, the energy of a dipole allowed transition $n \to n+1$ or $n+1 \to n$ is given by $E_n = 2\Delta + [(n+\gamma+1)+(n+\gamma)]\hbar\omega_c$ with $\gamma = 0$ for massive Dirac particles. This can be rewritten using the reduced exciton mass $\mu = m^*/2$ to give $E_n = 2\Delta + (n + 1/2)eB/\mu$. Equating the magnetic energy to $\hbar^2k^2/2\mu$ gives an expression for the k vector $k = \sqrt{2eB(n+1/2)/\hbar}$, which is equivalent to the Bohr-Sommerfeld quantization of area in k-space which is independent of the particle mass values assumed. In the plot of the observed transition energies versus $k = \sqrt{2eB(n+1/2)/\hbar}$, all the data collapse onto a single curve. The broken line in Fig. 2(b) shows a parabolic dispersion using a band gap $2\Delta = 0.2$ eV and reduced exciton mass μ=0.08m_0 (m_0 is the free electron mass). For energies above 0.6 eV a clear deviation from the simple parabolic model is observed reflecting the transition towards a $\sqrt{B}$ dependence for the energy of Dirac fermions, which is clearly visible in Fig. 2 (a). The reduced mass is consistent with recent results obtained by Shubnikov de Haas (SdH) measurements for n-type and p-type samples of Bi_2Se_3; the range of effective masses of the electrons and holes respectively is 0.12–0.16 m_0 and 0.23–0.25 m_0 in the literature,[13,21,22] corresponding to a value for the reduced mass, μ, in the range 0.079–0.098 m_0. It is also possible to estimate the effective masses from the Fermi velocity v_D and the electron-hole asymmetry term C using $m_e = 2\hbar^2/(\hbar^2 v_D^2/\Delta + 4C)$ and $m_h = 2\hbar^2/(\hbar^2 v_D^2/\Delta - 4C)$, giving $m_e = 0.138\,m_0$ and $m_h = 0.176\,m_0$, respectively.

Figure 3(a) shows the magneto-transmission of Bi_2Se_3 for temperatures from 7 to 300 K with an excitation

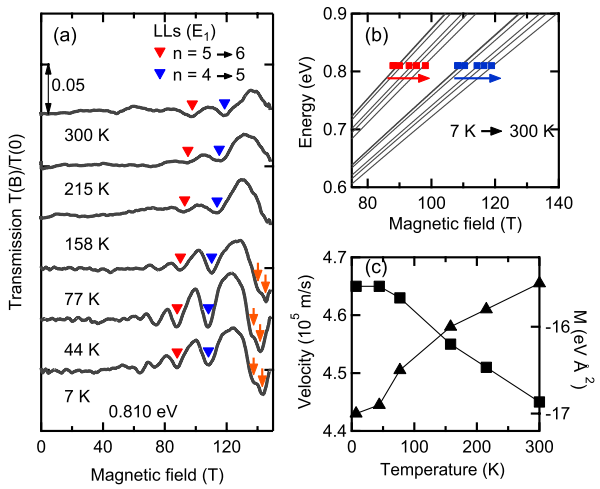

FIG. 3. (a) Magneto-transmittance of Bi_2Se_3 at the energy of 0.810 eV measured for different temperatures in fields up to 150 T. The position of the inter Landau level transitions are indicated by triangles. The splitting due to electron-hole asymmetry is indicated by arrows. The spectra have been shifted vertically for clarity. (b) Energy of transitions at 7 K and 300 K (symbols). The solid lines are fits to the Dirac like Hamiltonian. (c) Extracted Fermi velocity (squares) and negative mass parameter (triangles) versus temperature.

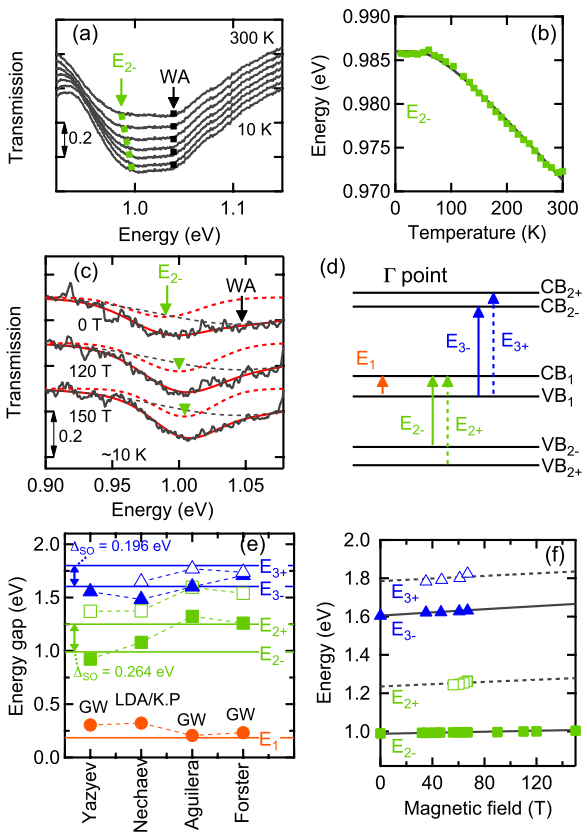

FIG. 4. (a) Transmission spectra of Bi_2Se_3 around 1.0 eV at 0 T at different temperatures of 10 and 50–300 K (50 K step). (b) Temperature dependence of 2^{nd} bandgap energy of Bi_2Se_3. Solid line is fitting by the expression in the text. (c) Low-temperature magneto-transmission spectra of Bi_2Se_3 at different magnetic fields. Spectra in (a) and (c) were shifted vertically for clarity and the weak feature labelled WA is due to water vapour absorption. (d) Schematic picture of band structure in the bulk of Bi_2Se_3 around the Γ point. (e) Low-temperature Landau fan chart of Bi_2Se_3 for 2^{nd} and 3^{rd} bandgaps and split-off bandgaps. Solid lines show the inter-band Landau levels obtained by the model described in the text.

energy of 0.810 eV. The inter band Landau level transitions of the fundamental band gap show a clear shift to higher magnetic fields with increasing temperatures. The observed shift cannot be attributed to a temperature dependence of the fundamental band gap energy 2Δ in the massive Dirac model as the avoided band crossing at low energies has almost no influence on the high energy inter band Landau level transitions. Instead we argue that this is due to a temperature dependence of the Fermi velocity and the negative mass parameter. In Fig. 3(b) we plot the observed transition energies at 7 and 300 K together with the transition energies calculated using the Dirac like Hamiltonian. From these we deduce, in Fig. 3(c), the temperature dependence of v_D and M. By 300 K the Fermi velocity has dropped to $v_D = 0.445\times10^6$ m s^{-1}, significantly ($\simeq 6\%$) lower than the low temperature value. At the same time the negative mass parameter has changed by around 10% to $M \simeq -15.5$ eVÅ^2 at 300K.

We now turn our attention to the transitions observed at higher energies in Fig. 1(a). There is clear evidence for a 2^{nd} band gap, with a pair of absorptions at 0.986 eV and 1.25 eV which we assign to a pair of transitions from a lower spin orbit split valance band[11] to the lowest empty conduction band (labeled $E_{2\pm}$). At still higher energies, we observe absorption from a second pair of transitions for the 3^{rd} band gap at 1.604 eV and 1.8 eV due to transitions (labeled $E_{3\pm}$) from the lowest occupied valence band to a higher spin orbit split conduction band. The observed optical transitions at the Γ point are shown schematically in Fig. 4(d). The transition energies (solid lines) are compared with the transition energies predicted by several LDA/GW band structure calculations[14,15,23,24] (symbols) shown in Fig. 4(e). The absolute values of the band gaps are in generally good agreement with theory and the spin-orbit splittings of the lower valence band (0.264 eV) and upper conduction band (0.196 eV) are also in good agreement with the predicted values. These higher band gaps are also consistent with those (1.0 eV and 1.6 eV) estimated from fitting the dielectric functions of bulk Bi_2Se_3 at 300 K as reported in Ref. 17, although the spin-orbit splitting could not be resolved.

We now examine the temperature and magnetic-field

dependence of the higher-energy absorptions. Figure 4 (a) shows the temperature dependence of the transmission spectra at temperatures of 10 K and 50 to 300 K (50 K step). The E_{2-} transition around 0.99 eV from the lower spin orbit split valence band (2^{nd} band gap) shows a clear shift towards higher energies with decreasing temperature, which is plotted in Fig. 4(b) (the small feature labelled WA is a water absorption around 1.04 eV.[25]) The temperature dependence was fitted using the well known expression for the temperature dependence of a semiconductor bandgap,[26]

$$E_g(T) = E_g(0) - S\langle\hbar\omega\rangle\left(\coth\left(\frac{\langle\hbar\omega\rangle}{2k_BT}\right) - 1\right), \quad (1)$$

where $E_g(T)$ is the band gap at the temperature T with $E_g(0) = 0.986$ eV, $S = 0.423$ is a dimensionless coupling constant and $\langle\hbar\omega\rangle = 19.4$ meV is the average phonon energy (see Fig. S3 for the temperature dependence of 1.6 eV absorption). The average phonon energy is within the range of optical phonon energies (4.6–21.6 meV) seen in Raman spectroscopy in the literature.[27]

Figure 4(c) shows the magnetic field dependence of the transmission spectra, $T(B)$, at 0, 120 and 150 T, measured using a super-continuum light source (white-light laser) in the range 1.1 to 1.7 m. A single 20ns light pulse is synchronized with the magnetic field pulse from the single turn coil and the spectrometer acquisition window. The light pulse is beamsplit and the sample transmission normalised against the same pulse to account for pulse to pulse variability. The E_{2-} around 0.99 eV at 0 T shows a small but clear shift towards higher energy with increasing magnetic fields (∼15 meV shift at 150 T) and a field induced increase in intensity. This small diamagnetic shift compared with that of ∼100 meV (Fig. 2) seen for the fundamental band gap is consistent with the assignment of this transition as a strongly bound excitonic state associated with the second band gap. The increase in intensity and shift produced by the magnetic field also result in the strong differential transmission signals seen in Fig. 1 for the $E_2^{\pm}$ and $E_3^{\pm}$ transitions, which allows them to be distinguished from the higher quantum number interband Landau level transitions of band gap E_1 seen in a similar energy range in Fig. 1(a).

The relative strenghts of the band edge E_{2-} transition and the higher landau level E_1 transitions can be seen in Fig. 1(b) from the magnetic field dependent transmission in the 100T range of magnetic fields at 1.0 eV where changes as large as 20% can be seen, compared to the few % changes for the higher Landau levels. This is further evidence that the E_{2-} and E_{3-} transitions are not high-order Landau levels of the fundamental band gap, but the lowest interband Landau level transitions of the 2^{nd} and 3^{rd} band gaps with intensities enhanced by excitonic interactions. Such behavior is typical of that seen, for example, in magneto-transmission studies in the 100T range of magnetic fields for excitonic states in GaSe[28] and the organic lead halide perovskite $CH_3NH_3PbI_3$.[29]

The exciton diamagnetic shift can be used to estimate some properties of the higher band gap excitonic states using the expression,[30,31]

$$\Delta E_g(B) = \frac{e^2\langle r^2\rangle B^2}{8\mu}, \quad (2)$$

which does not require a knowledge of the dielectric constant and where r is the size of the exciton wavefunction and μ is the exciton reduced effective mass between the CB_1 and VB_{2-} interband transitions. Recent recent **k.p** calculations[23] suggest that the effective masses in the lower valuence band and upper conduction bands will be comparable to those for CB_1 and VB_1, allowing us to approximate μ to be on the order of μ=0.1 m_0. This means that Eq.2 predicts that the exciton size is only on the order of $\sqrt{\langle r^2\rangle}$= 1.8 nm. This seems surprisingly small given the well know high values for the dielectric constant of Bi_2Se_3, which has been shown to be of order 30 even up to photon energies as high as 2 eV.[17] However such a value would be consistent with the idea that there is be a significant excitonic contribution to these higher band transitions which influences the band edge absorption.

In conclusion we have used magnetospectroscopy over a wide range of energies (0.55 to 2.2 eV) and magnetic fields up to 150 T to investigate the bulk band structure of the topological insulator Bi_2Se_3. The interband Landau level transitions of the fundamental bandgap are observed to deviate from the previously reported[16] linearity at high-energies, but can be described by a 4×4 massive Dirac Hamiltonian with a negative mass term arising from band inversion caused by strong spin-orbit coupling. Furthermore, in high magnetic fields the differential absorption spectra, $T(B)/T(0)$, reveal new strong resonances which were assigned as the lowest interband Landau level transitions of the 2^{nd} and 3^{rd} bandgaps observed at high energies around 0.99 and 1.6 eV, with clearly resolved spin-orbit splittings. From their temperature and magnetic-field dependence, they were assigned as excitonic band edge transitions for these higher bandgaps.

I. ACKNOWLEDGEMENTS

This work was supported by EPSRC (UK) via its membership of the EMFL (grant no. EP/N01085X/1), the TERASPEC project of the Emergence program of IDEX Toulouse, and MEGATER project funded by NEXT Toulouse, by ANR JCJC project milliPICS, the Région Midi-Pyrénées under contract MESR 13053031, the BLAPHENE and STRABOT projects under IDEX program Emergence, and by "Programme Investissements d'Avenir" under the program ANR-11-IDEX-0002-02, reference ANR-10-LABX-0037-NEXT. This work arises from research funded by the John Fell Oxford University Press Research Fund. LBD acknowledges financial support from EPSRC and the Science and Technology Facilities Council (UK).

* r.nicholas@physics.ox.ac.uk

[1] M. Z. Hasan and C. L. Kane, Rev. Mod. Phys. **82**, 3045 (2010).
[2] X.-L. Qi and S.-C. Zhang, Rev. Mod. Phys. **83**, 1057 (2011).
[3] Y. Ando, J. Phys. Soc. Japan **82**, 102001 (2013).
[4] A. R. Mellnik, J. S. Lee, A. Richardella, J. L. Grab, P. J. Mintun, M. H. Fischer, A. Vaezi, A. Manchon, E.-A. Kim, N. Samarth, and D. C. Ralph, Nature **511**, 449 (2014).
[5] K. Kondou, R. Yoshimi, A. Tsukazaki, Y. Fukuma, J. Matsuno, K. S. Takahashi, M. Kawasaki, Y. Tokura, and Y. Otani, Nat Phys **12**, 1027 (2016).
[6] Y. Xia, D. Qian, D. Hsieh, L. Wray, A. Pal, H. Lin, A. Bansil, D. Grauer, Y. S. Hor, R. J. Cava, and M. Z. Hasan, Nat Phys **5**, 398 (2009).
[7] D. Hsieh, Y. Xia, D. Qian, L. Wray, J. H. Dil, F. Meier, J. Osterwalder, L. Patthey, J. G. Checkelsky, N. P. Ong, A. V. Fedorov, H. Lin, A. Bansil, D. Grauer, Y. S. Hor, R. J. Cava, and M. Z. Hasan, Nature **460**, 1101 (2009).
[8] Y. L. Chen, J. G. Analytis, J.-H. Chu, Z. K. Liu, S.-K. Mo, X. L. Qi, H. J. Zhang, D. H. Lu, X. Dai, Z. Fang, S. C. Zhang, I. R. Fisher, Z. Hussain, and Z.-X. Shen, Science **325**, 178 (2009).
[9] D. Hsieh, Y. Xia, D. Qian, L. Wray, F. Meier, J. H. Dil, J. Osterwalder, L. Patthey, A. V. Fedorov, H. Lin, A. Bansil, D. Grauer, Y. S. Hor, R. J. Cava, and M. Z. Hasan, Phys. Rev. Lett. **103**, 146401 (2009).
[10] H. Zhang, C.-X. Liu, X.-L. Qi, X. Dai, Z. Fang, and S.-C. Zhang, Nat Phys **5**, 438 (2009).
[11] C.-X. Liu, X.-L. Qi, H. Zhang, X. Dai, Z. Fang, and S.-C. Zhang, Phys. Rev. B **82**, 045122 (2010).
[12] K. W. Post, B. C. Chapler, L. He, X. Kou, K. L. Wang, and D. N. Basov, Phys. Rev. B **88**, 075121 (2013).
[13] B. A. Piot, W. Desrat, D. K. Maude, M. Orlita, M. Potemski, G. Martinez, and Y. S. Hor, Phys. Rev. B **93**, 155206 (2016).
[14] O. V. Yazyev, E. Kioupakis, J. E. Moore, and S. G. Louie, Phys. Rev. B **85**, 161101 (2012).
[15] I. Aguilera, C. Friedrich, G. Bihlmayer, and S. Blügel, Phys. Rev. B **88**, 045206 (2013).
[16] M. Orlita, B. A. Piot, G. Martinez, N. K. S. Kumar, C. Faugeras, M. Potemski, C. Michel, E. M. Hankiewicz, T. Brauner, C. Drasar, S. Schreyeck, S. Grauer, K. Brunner, C. Gould, C. Brüne, and L. W. Molenkamp, Phys. Rev. Lett. **114**, 186401 (2015).
[17] M. Eddrief, F. Vidal, and B. Gallas, Journal of Physics D: Appl. Phys. **49**, 505304 (2016).
[18] L. Collins-McIntyre, M. Watson, A. Baker, S. Zhang, A. Coldea, S. Harrison, A. Pushp, A. Kellock, S. Parkin, G. van der Laan, and T. Hesjedal, AIP Advances **4**, 127136 (2014).
[19] L. Collins-McIntyre, W. Wang, B. Zhou, S. Speller, Y. Chen, and T. Hesjedal, Phys. Stat. Solidi B **252**, 1334 (2015).
[20] R. J. Nicholas, P. Y. Solane, and O. Portugall, Phys. Rev. Lett. **111**, 096802 (2013).
[21] K. Eto, Z. Ren, A. A. Taskin, K. Segawa, and Y. Ando, Phys. Rev. B **81**, 195309 (2010).
[22] J. G. Analytis, J.-H. Chu, Y. Chen, F. Corredor, R. D. McDonald, Z. X. Shen, and I. R. Fisher, Phys. Rev. B **81**, 205407 (2010).
[23] I. A. Nechaev and E. E. Krasovskii, Phys. Rev. B **94**, 201410 (2016).
[24] T. Förster, P. Krüger, and M. Rohlfing, Phys. Rev. B **92**, 201404 (2015).
[25] J. R. Collins, Phys. Rev. **26**, 771 (1925).
[26] K. P. ODonnell and X. Chen, Appl. Phys. Lett. **58**, 2924 (1991).
[27] J. Zhang, Z. Peng, A. Soni, Y. Zhao, Y. Xiong, B. Peng, J. Wang, M. S. Dresselhaus, and Q. Xiong, *Nano Letters*, Nano Lett. **11**, 2407 (2011).
[28] K. Watanabe, K. Uchida, and N. Miura, Phys. Rev. B **68**, 155312 (2003).
[29] A. Miyata, A. Mitioglu, P. Plochocka, O. Portugall, J. T.-W. Wang, S. D. Stranks, H. J. Snaith, and R. J. Nicholas, Nat Phys **11**, 582 (2015).
[30] N. Miura, *Physics of Semiconductors in High Magnetic Fields* (Oxford Univ. Press, 2008).
[31] S. N. Walck and T. L. Reinecke, Phys. Rev. B **57**, 9088 (1998).